Acta Cryst. (1975). **B31**, 1293

The Crystal Structures of Caesium Pentamolybdate, $Cs_2Mo_5O_{16}$, and Caesium Heptamolybdate, $Cs_2Mo_7O_{22}$

By B. M. Gatehouse and B. K. Miskin

Department of Chemistry, Monash University, Clayton, Victoria, Australia, 3168

(*Received* 12 *December* 1974; *accepted* 16 *December* 1974)

Caesium pentamolybdate and caesium heptamolybdate both crystallize in the monoclinic space group $C2/c$ with $a=21{\cdot}44$, $b=5{\cdot}559$, $c=14{\cdot}338$ Å, $\beta=122{\cdot}74°$ for the former and $a=21{\cdot}54$, $b=5{\cdot}537$, $c=18{\cdot}91$ Å, $\beta=122{\cdot}71°$ for the latter. Both compounds have $Z=4$; the measured and calculated densities are 4·62 and 4·63 g cm^{-3} respectively for the pentamolybdate and 4·55 and 4·514 gm cm^{-3} for the heptamolybdate. Of the 3150 unique, counter intensities collected for the pentamolybdate, 2999 with $I>3\sigma(I)$ were used in the solution and refinement of the structure to $R=0{\cdot}041$ ($R_w=0{\cdot}076$), although 17 of these were considered to be seriously extinguished and were given zero weight. For the heptamolybdate 2744 reflexions were collected in a similar manner and 1762 of these with $I>3\sigma(I)$ were used in the solution and refinement of the structure to $R=0{\cdot}039$ ($R_w=0{\cdot}043$). The two structures are very similar; both are composed of sheets of linked Mo–O octahedra joined by Cs–O polyhedra. The Mo–O framework is composed of strips of MoO_3-type structure joined at twofold axes, the composition of the structure being dependent on the number of Mo–O octahedra between the twofold axes.

Introduction

This work originated from an attempt to prepare and determine the structure of $Cs_2Mo_4O_{13}$, a phase which was reported by Spitsyn & Kuleshov (1951) and Salmon & Caillet (1969). It was of interest to compare the structure of this compound with that of $Rb_2Mo_4O_{13}$ and isomorphous $K_2Mo_4O_{13}$ (Gatehouse & Leverett, 1971). During the initial stages it became obvious that the compound being studied was $Cs_2Mo_5O_{16}$ and not the tetramolybdate. The structure of the pentamolybdate which is reported here suggested the existence of a series of structures of varying composition based on a similar motif. The structure of the heptamolybdate, a phase not reported by earlier workers but which was reported by Hoekstra (1973), confirmed this view and is also reported here. A brief report of these structures has been published elsewhere (Gatehouse, 1974).

Experimental

Preliminary studies of the crystalline products of slowly cooled melts of Cs_2CO_3 and MoO_3 in the mole ratios $1:x$ ($4\le x\le 10$) revealed the presence of two crystalline phases, $Cs_2Mo_5O_{16}$ and $Cs_2Mo_7O_{22}$. This contradicted the work of Spitsyn & Kuleshov (1951), who reported the hexa- and octamolybdates, and that of Salmon & Caillet (1969) who correctly reported the pentamolybdate but who believed the other phase to be $Cs_2Mo_9O_{28}$. Both these groups reported the tetramolybdate but single crystals could not be prepared during this study. The paper on the Cs_7MoO_4–MoO_3 system by Hoekstra (1973), which was received after the completion of this work, has described the complex behaviour of the system in the tetramolybdate region.

The densities of the penta- and heptamolybdates (Table 1) were determined pycnometrically with powdered samples prepared by triturating the appropriate ratios of Cs_2MoO_4 and MoO_3 and heating to 450–480 °C for about 20 h, grinding the white, microcrystalline product and then reheating for a further 20 to 24 h.

Table 1. *Crystallographic data for* $Cs_2Mo_5O_{16}$, $Cs_2Mo_7O_{22}$ *and* $Rb_2Mo_7O_{22}$

	$Cs_2Mo_5O_{16}$	$Cs_2Mo_7O_{22}$	$Rb_2Mo_7O_{22}$
Crystal system	Monoclinic	Monoclinic	Monoclinic
Space group	$C2/c$	$C2/c$	$C2/c$
a (Å)	21·44 (1)	21·54 (1)	20·73 (1)
b (Å)	5·559 (3)	5·537(3)	5·553 (3)
c (Å)	14·338 (7)	18·91 (1)	18·56 (1)
β (°)	122·74 (4)	122·71 (3)	120·79 (5)
V (Å)^3	1438 (3)	1897 (3)	1836 (3)
Z	4	4	4
D_c (g cm^{-3})	4·63 (1)	4·514 (7)	4·32 (1)
D_m (g cm^{-3})	4·62 (3)	4·55 (3)	4·29 (3)
μ(Mo $K\alpha$) (cm^{-1})	93·0	83·3	

Caesium pentamolybdate

Determination of the unit cell

A crystal with a distorted cubic shape and an average thickness of about 0·025 mm ($\mu R\simeq 1{\cdot}16$) was chosen from a melt of Cs_2CO_3 and MoO_3 in the mole ratio 1:4. Weissenberg photography with Cu $K\alpha$ radiation showed that the compound was monoclinic with space group $C2/c$ or Cc.

The crystal was mounted on a Philips PW1100 automatic four-circle diffractometer (courtesy of Dr E. Keulen, Philips' Research Laboratories, Eindhoven, Holland) and the cell dimensions reported in Table 1 were obtained by least-squares refinement of cell and orientation parameters from the positions of 25 reasonably intense reflexions. Graphite-monochromated Mo $K\alpha$ radiation ($\lambda = 0{\cdot}7107$ Å) was used.

Intensity data

Graphite-monochromated Mo $K\alpha$ radiation was also used for the collection of intensities. 3150 unique reflexions with $2{\cdot}0 \le \theta \le 35{\cdot}0$ and $k, l \ge 0$ were monitored by θ–2θ scans with constant width, $\Delta\theta = 1{\cdot}5°$, and a speed of $0{\cdot}025°\ \mathrm{s}^{-1}$. At each extreme of the scan a background count was measured for half the scan time. Three non-coplanar reference reflexions were measured every two hours and no systematic variations in their intensities were detected. The variance of an observed intensity, I, was calculated from

$$\sigma^2(I) = \sigma^2(C) + \sigma^2(B_1) + \sigma^2(B_2) + (0{\cdot}04I)^2$$

where C was the peak intensity without correction for background and B_1 and B_2 were the two background counts. The factor 0·04 was taken as the average error in a strong reflexion.

The observed intensities and their variances were corrected for Lorentz and polarization effects. Since the plane of reflexion of the specimen was perpendicular to that of the monochromator

$$(\mathrm{Lp})^{-1} = \sin 2\theta\,(1 + \cos^2 2\theta_m)/(\cos^2 2\theta + \cos^2 2\theta_m)$$

where $\theta_m = 6{\cdot}08°$ was the Bragg angle of the monochromator. The absorption correction for a sphere with $\mu R = 1{\cdot}16$ was also applied (*International Tables for X-ray Crystallography*, 1959). The corrected intensities, F^2, were reduced to observed structure amplitudes, F, and the standard deviation of F was calculated from

$$\sigma(F) = \sigma(F^2)/2F\,.$$

228 weak reflexions with $I \le 3\sigma(I)$ were given zero weight in the structure solution and refinement.

Scattering factors and programs

The scattering factors for Cs^+, Mo^0 and O^0 were those of Cromer & Waber (1965). All computing was performed on the Monash University CDC 3200 computer. The major programs were *MONLS*, a modified version of the full-matrix least-squares program of Busing, Martin & Levy (1962), *MONDLS*, a block-diagonal least-squares program adapted from the 'SF' series of Shiono (1968) and the Fourier summation program, *MONFR* (White, 1965).

Structure solution

The centrosymmetric space group $C2/c$ was chosen for solving the structure and the subsequent satisfactory refinement of the structure confirmed this choice. The heavy-atom structure was solved by conventional Harker techniques and the oxygen positions were found from subsequent difference maps.

A number of cycles of full-matrix least-squares refinement of the isotropic model, with all 'observed' data given unit weights, reduced $R = \sum||F_o| - |F_c||/\sum|F_o|$ to 0·085. Use of the block-diagonal least-squares technique, with reflexions weighted by $1/\sigma^2(F)$ and with

Table 2. *Final positional and thermal parameters for* $\mathrm{Cs_2Mo_5O_{16}}$ *and* $\mathrm{Cs_2Mo_7O_{22}}$

B is the Debye–Waller temperature factor. The anisotropic temperature factor is of the form $\exp\,[-2\pi^2(U_{11}h^2a^{*2} + U_{22}k^2b^{*2} + U_{33}l^2c^{*2} + 2U_{12}hka^*b^* + 2U_{13}hla^*c^* + 2U_{23}klb^*c^*) \times 10^{-4}]$. Estimated standard deviations are in parentheses.

Caesium pentamolybdate

	x	y	z	U_{11}	U_{22}	U_{33}	U_{12}	U_{13}	U_{23}
Mo(1)	0	0·1350 (2)	0·25	101 (5)	68 (4)	88 (5)	0	58 (4)	0
Mo(2)	0·10958 (5)	0·7831 (2)	0·46280 (7)	76 (3)	89 (4)	104 (3)	−1 (3)	53 (3)	18 (3)
Mo(3)	0·06128 (5)	0·3288 (2)	0·60782 (7)	72 (3)	73 (4)	91 (3)	1 (3)	49 (3)	14 (3)
Cs	0·22113 (5)	0·1616 (2)	0·33569 (8)	227 (4)	209 (4)	337 (5)	13 (3)	195 (4)	38 (3)

	x	y	z	B		x	y	z	B
O(1)	0·0995 (4)	0·039 (2)	0·3676 (6)	0·9 (1)	O(5)	0·0571 (4)	0·604 (2)	0·5184 (7)	1·0 (1)
O(2)	0·0724 (5)	0·102 (2)	0·5368 (7)	1·3 (2)	O(6)	0·0286 (5)	0·674 (2)	0·6868 (7)	1·1 (1)
O(3)	0·0087 (5)	0·178 (2)	0·6616 (6)	0·8 (1)	O(7)	0·1907 (5)	0·846 (2)	0·5854 (8)	1·5 (2)
O(4)	0·1362 (5)	0·549 (2)	0·4154 (7)	1·5 (2)	O(8)	0·1494 (5)	0·367 (2)	0·7226 (8)	1·4 (1)

Caesium heptamolybdate

	x	y	z	U_{11}	U_{22}	U_{33}	U_{12}	U_{13}	U_{23}
Mo(1)	0·5	0·1173 (3)	0·25	82 (8)	60 (9)	77 (8)	0	24 (7)	0
Mo(2)	0·18908 (7)	0·1884 (3)	0·02696 (8)	72 (6)	66 (6)	90 (6)	−17 (5)	35 (5)	−12 (5)
Mo(3)	0·03472 (7)	0·2499 (3)	0·40618 (8)	83 (6)	91 (6)	96 (6)	17 (5)	43 (5)	13 (5)
Mo(4)	0·16252 (7)	0·1432 (3)	0·36241 (8)	70 (5)	63 (6)	79 (5)	11 (5)	31 (5)	12 (5)
Cs	0·34516 (6)	0·1559 (2)	0·32331 (8)	168 (5)	232 (6)	271 (6)	23 (5)	120 (5)	38 (5)

	x	y	z	B		x	y	z	B
O(1)	0·0265 (6)	0·021 (2)	0·1423 (7)	1·5 (2)	O(7)	0·0743 (5)	0·301 (2)	0·3193 (7)	0·9 (2)
O(2)	0·4821 (6)	0·018 (2)	0·3347 (7)	1·1 (2)	O(8)	0·0336 (7)	0·295 (2)	0·4941 (7)	1·8 (2)
O(3)	0·3710 (6)	0·077 (2)	0·0212 (7)	1·5 (2)	O(9)	0·4245 (6)	0·307 (2)	0·1967 (7)	1·2 (2)
O(4)	0·1301 (6)	0·076 (2)	0·4570 (7)	1·0 (2)	O(10)	0·2259 (6)	0·367 (2)	0·4192 (7)	1·2 (2)
O(5)	0·1749 (6)	0·105 (3)	0·2813 (7)	1·5 (2)	O(11)	0·2808 (5)	0·363 (2)	0·0667 (6)	1·0 (2)
O(6)	0·1924 (6)	0·153 (2)	0·1189 (7)	1·6 (2)					

the metal atoms varying anisotropically and the oxygens isotropically, reduced R to 0·052 and $R_w = (\sum w(|F_o|-|F_c|)^2/\sum wF_o^2)^{1/2}$ from 0·103 to 0·087.

At this stage the distribution of R_w against $\sin\theta/\lambda$ was generally level for $\sin\theta/\lambda > 0{\cdot}3$ but increased sharply below this value. A number of intense, low-angle reflexions showed discrepancies between F_o and F_c which could probably be best attributed to extinction. The 17 worst affected reflexions, with $F_c > 150$, $\sin\theta/\lambda < 0{\cdot}3$ and $(F_c-F_o)/F_o > 0{\cdot}1$, were rejected. Block-diagonal least-squares refinement then reduced R to 0·038, R_w to 0·075, and resulted in a more satisfactory distribution of R_w against $\sin\theta/\lambda$. At this stage all shifts were below 0·1σ and the refinement was terminated. The final positional and thermal parameters are reported in Table 2.*

A difference synthesis showed some significant fea-

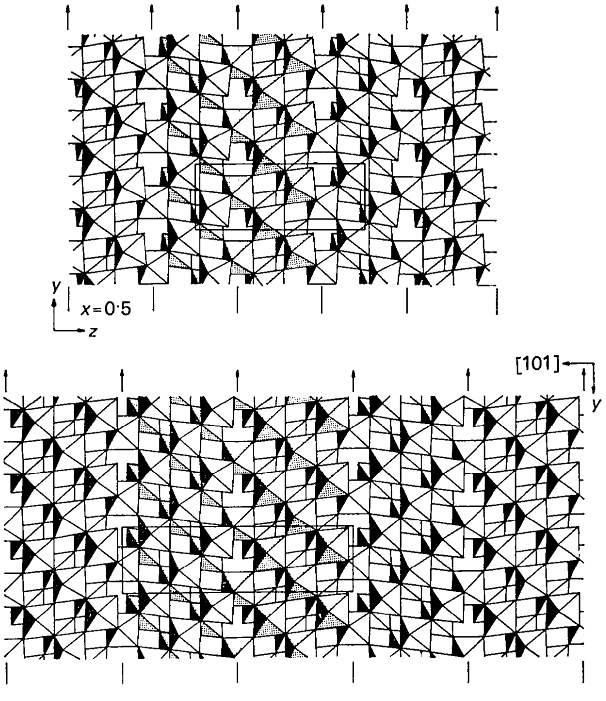

Fig. 1. The sheet of octahedra which forms the Mo–O framework in $Cs_2Mo_5O_{16}$ (above) and $Cs_2Mo_7O_{22}$ (below) viewed perpendicular to the mean plane of the sheet. Twofold axes are denoted by arrows. One of the ReO_3-type strips is shaded for clarity. MoO_3-type strips can be seen between the twofold axes: these are $2\frac{1}{2}$ octahedra wide in the pentamolybdate and $3\frac{1}{2}$ octahedra wide in the heptamolybdate. The corners of the rectangles enclosing the repeating units have the coordinates $\frac{1}{2},0,0$; $\frac{1}{2},1,0$; $\frac{1}{2},1,1$; $\frac{1}{2},0,1$ (above) and $0,0,\frac{1}{4}$; $0,1,\frac{1}{4}$; $1,1,1\frac{1}{4}$; $1,0,1\frac{1}{4}$ (below).

Table 3. *Selected interatomic distances* (Å) *in caesium pentamolybdate and caesium heptamolybdate*

The symmetry transformations are indicated by the superscripts. The roman numerals refer to the symmetry transformations as follows: I (x,y,z), II $(\bar{x},\bar{y},\bar{z})$, III $(\bar{x},y,\frac{1}{2}-z)$, IV $(x,\bar{y},\frac{1}{2}+z)$, V $(\frac{1}{2}+x,\frac{1}{2}+y,z)$, VI $(\frac{1}{2}-x,\frac{1}{2}-y,\bar{z})$, VII $(\frac{1}{2}-x,\frac{1}{2}+y,\frac{1}{2}-z)$. The absence of a roman numeral indicates no symmetry transformation, *i.e.* (x,y,z). If the atom referred to occurs in a cell adjacent to the primary unit cell, the relationship of that cell to the primary cell is given by a (0, +1,0), b(−1,0,0), c(0, −1,0), d(0,0, −1), e(−1, −1,0), f(0, −1, −1).

Estimated standard deviations are in parentheses.

(*a*) Mo–Mo edge-shared octahedra

$Cs_2Mo_5O_{16}$		$Cs_2Mo_7O_{22}$	
Mo(1)–Mo(2)^{c}	3·302 (2)	Mo(1)–Mo(3)$^{\mathrm{V}c}$	3·321 (2)
Mo(2)–Mo(3)$^{\mathrm{II}b}$	3·290 (2)	Mo(2)–Mo(2)$^{\mathrm{VI}d}$	3·359 (3)
Mo(3)–Mo(3)$^{\mathrm{II}b}$	3·361 (2)	–Mo(4)$^{\mathrm{IV}f}$	3·384 (2)
		Mo(3)–Mo(4)	3·327 (3)

(*b*) Mo–Mo corner-shared octahedra

$Cs_2Mo_5O_{16}$		$Cs_2Mo_7O_{22}$	
Mo(1)–Mo(3)$^{\mathrm{II}e}$	3·928 (2)	Mo(1)–Mo(4)$^{\mathrm{V}c}$	3·952 (2)
–Mo(3)$^{\mathrm{II}b}$	4·203 (2)	–Mo(4)$^{\mathrm{V}}$	4·148 (2)
Mo(2)–Mo(3)	3·755 (2)	Mo(2)–Mo(4)$^{\mathrm{VII}}$	3·702 (2)
–Mo(3)^{a}	4·114 (2)	–Mo(3)$^{\mathrm{IV}f}$	3·735 (2)
		–Mo(4)$^{\mathrm{VII}c}$	4·059 (2)
		–Mo(3)$^{\mathrm{IV}d}$	4·211 (2)

(*c*) Mo–O

$Cs_2Mo_5O_{16}$		$Cs_2Mo_7O_{22}$	
Mo(1)–O(6)$^{\mathrm{II}b,\,\mathrm{IV}}$	1·710 (11)	Mo(1)–O(9)$^{\mathrm{I},\,\mathrm{III}}$	1·730 (11)
–O(1)$^{\mathrm{I},\,\mathrm{III}b}$	1·947 (7)	–O(2)$^{\mathrm{I},\,\mathrm{III}}$	1·918 (14)
–O(3)$^{\mathrm{II}e,\,\mathrm{IV}c}$	2·219 (9)	–O(7)$^{\mathrm{V}c,\,\mathrm{VII}c}$	2·255 (10)
Mo(2)–O(4)	1·704 (11)	Mo(2)–O(3)$^{\mathrm{VI}d}$	1·707 (11)
–O(7)	1·712 (8)	–O(6)	1·712 (15)
–O(1)^{a}	1·901 (9)	–O(4)$^{\mathrm{IV}f}$	1·920 (10)
–O(5)	1·965 (11)	–O(11)	1·949 (12)
–O(3)$^{\mathrm{II}b}$	2·184 (7)	–O(11)$^{\mathrm{VI}d}$	2·209 (15)
–O(2)^{a}	2·411 (11)	–O(10)$^{\mathrm{VII}c}$	2·355 (11)
Mo(3)–O(2)	1·718 (10)	Mo(3)–O(1)$^{\mathrm{III}b}$	1·697 (11)
–O(8)	1·721 (7)	–O(8)	1·694 (16)
–O(3)	1·873 (11)	–O(2)$^{\mathrm{V}b}$	1·913 (11)
–O(5)	1·968 (9)	–O(4)	1·985 (11)
–O(5)$^{\mathrm{II}b}$	2·211 (7)	–O(7)	2·239 (15)
–O(6)	2·514 (10)	–O(3)$^{\mathrm{VII}}$	2·506 (11)
		Mo(4)–O(5)	1·705 (16)
		–O(10)	1·721 (11)
		–O(7)	1·833 (11)
		–O(11)$^{\mathrm{VII}c}$	1·982 (10)
		–O(4)	2·275 (15)
		–O(9)$^{\mathrm{VII}c}$	2·442 (11)

(*d*) Cs–O less than 4·0 Å

$Cs_2Mo_5O_{16}$		$Cs_2Mo_7O_{22}$	
Cs–O(1)	2·961 (10)	Cs–O(2)	2·941 (13)
–O(8)$^{\mathrm{IV}}$	3·027 (9)	–O(8)$^{\mathrm{VI}}$	3·011 (10)
–O(7)$^{\mathrm{VI}}$	3·168 (9)	–O(5)$^{\mathrm{VII}}$	3·061 (13)
–O(7)$^{\mathrm{VI}c}$	3·241 (9)	–O(1)$^{\mathrm{VII}}$	3·195 (13)
–O(7)$^{\mathrm{IV}}$	3·282 (12)	–O(6)$^{\mathrm{VII}}$	3·221 (14)
–O(8)$^{\mathrm{VI}}$	3·308 (13)	–O(6)$^{\mathrm{VII}c}$	3·250 (14)
–O(8)$^{\mathrm{IV}c}$	3·306 (9)	–O(5)	3·317 (14)
–O(4)	3·393 (12)	–O(6)	3·466 (9)
–O(4)$^{\mathrm{VI}c}$	3·414 (8)	–O(5)$^{\mathrm{VII}c}$	3·531 (13)
–O(6)$^{\mathrm{IV}}$	3·592 (9)	–O(3)$^{\mathrm{IV}c}$	3·704 (14)
–O(2)$^{\mathrm{IV}c}$	3·987 (10)	–O(9)	3·710 (15)
–O(2)$^{\mathrm{VI}}$	3·990 (10)		

(*e*) Cs–Cs

$Cs_2Mo_5O_{16}$		$Cs_2Mo_7O_{22}$	
Cs–Cs$^{\mathrm{VI}}$	4·294 (2)	Cs–Cs$^{\mathrm{VII},\,\mathrm{VII}c}$	4·457 (2)
–Cs$^{\mathrm{VII},\,\mathrm{VII}c}$	4·308 (2)	–Cs$^{a,\,c}$	5·537 (3)
–Cs$^{a,\,c}$	5·559 (3)		

---

* Lists of observed and calculated structure factors for both this structure and that of caesium heptamolybdate have been deposited with the British Library Lending Division as Supplementary Publication No. SUP 30827 (45 pp., 1 microfiche). Copies may be obtained through The Executive Secretary, International Union of Crystallography, 13 White Friars, Chester CH1 1NZ, England.

tures. At the four heavy-atom positions the electron density ranged between $-1{\cdot}5$ and $-3{\cdot}0$ e Å^{-3}. Each position was surrounded by areas of positive density (as high as 2·2 e Å^{-3} in some cases) about 1 Å from the centre. These features were probably associated with extinction and differential absorption effects. Elsewhere the electron density was between ± 1 e Å^{-3}.

Description of the structure

The structure of $Cs_2Mo_5O_{16}$ is composed of sheets of Mo–O octahedra linked to each other by sheets of Cs–O polyhedra. The basic unit of the Mo–O framework could be considered to be a block of ReO_3-type structure which is five octahedra wide, one octahedron deep and of infinite length. Each such block joins with two other identical blocks by sharing octahedron edges to form a 'staggered sheet' as shown in Fig. 1. A *b*-axis projection of the structure is shown in Fig. 2.

The Mo–O octahedra show the distortions which are typical of that species (Gatehouse & Miskin, 1974). The Mo–O distances lie between 1·70 and 2·51 Å with average distances of 1·96, 1·98 and 2·00 Å for the octahedra about Mo(1), Mo(2) and Mo(3) respectively. Pertinent interatomic distances are reported in Table 3.

In this structure Cs is coordinated by ten oxygens (Fig. 3). On one side Cs is surrounded by a pentagon formed by O(1), O(8)^{IVc}, O(7)^{IV}, O(8)^{IV} and O(4), and on the other by a distorted square; O(7)^{VI}, O(8)^{VI}, O(7)^{VIc} and O(4)^{VIc}. These oxygens lie between 2·96 and 3·41 Å from Cs. O(6)^{IV} is 3·59 Å from Cs through the pentagonal face and may be considered to be coordinated. Cs–O(2)^{IVc} is 3·99 Å, also through the pentagonal face, and Cs–O(2)^{VI} is the same distance through the square face but this distance is probably too long for the oxygens to be considered as coordinated. The pentagon and the square of oxygens are arranged so that two other square faces are formed. These two faces, O(8)^{IV}–O(7)^{VI}–O(8)^{VI}–O(7)^{IV} and O(7)^{IV}–O(8)^{VI}–O(7)^{VIc}–O(8)^{IVc} are shared with other Cs–O polyhedra to form chains which share O(4) and O(4)^{VIc} with adjacent chains to give rise to sheets of Cs–O polyhedra.

Caesium heptamolybdate

Determination of the unit cell

A small prism with dimensions 0·025 × 0·028 × 0·033 mm was mounted about the prism axis on Monash University's Philips PW1100 automatic four-circle diffractometer. Graphite-monochromated Mo $K\alpha$ radiation ($\lambda = 0{\cdot}7107$ Å) with a take-off angle of 6° and monochromator angle, $\theta_m = 5{\cdot}94°$, was used. A least-squares refinement of cell and orientation parameters with 25 reasonably intense reflexions yielded the cell dimensions listed in Table 1.

An examination of a set of rapidly collected low-angle data indicated that the space group was either *C*2/*c* or *Cc*. Subsequent examination of the complete data set confirmed this conclusion.

Intensity data

Intensities were collected by θ–2θ scans with width, $\Delta\theta = 1{\cdot}0°$, and a speed of 0·0168° s^{-1}. The method of counting the background was the same as in the pen-

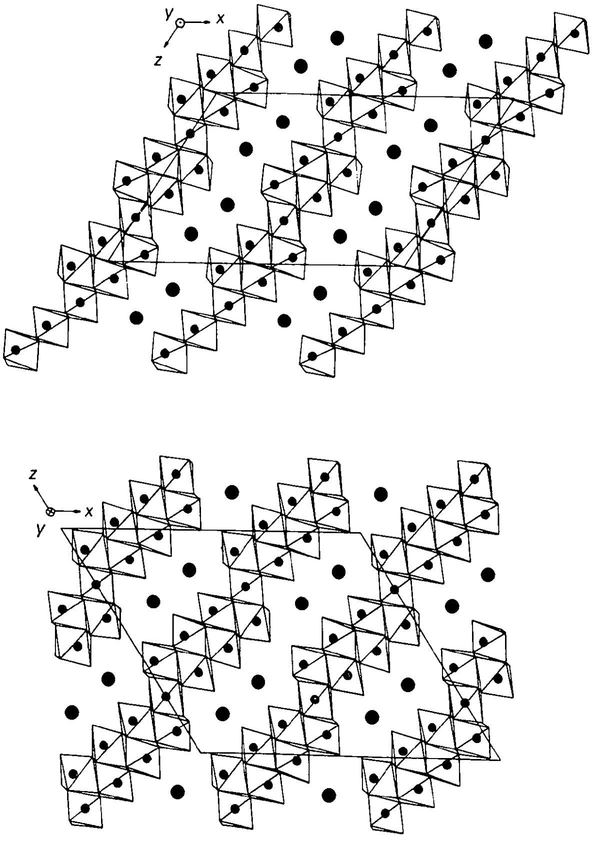

Fig. 2. Projections along the *b* axes of $Cs_2Mo_5O_{16}$ (above) and $Cs_2Mo_7O_{22}$ (below). The unit-cell outlines are shown. Large filled circles represent Cs positions while the small filled circles within the octahedra represent Mo positions. Two-fold axes are at $0,y,\frac{1}{4}$; $0,y,\frac{3}{4}$, $\frac{1}{2},y,\frac{1}{4}$ and $\frac{1}{2},y,\frac{3}{4}$. Note how the positions of the Mo–O sheets relative to each other and the positions of the Cs atoms relative to the sheets are almost identical in the two structures.

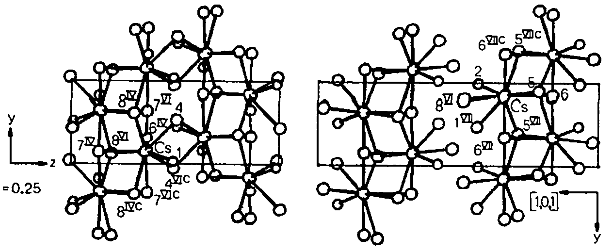

Fig. 3. The sheets of Cs–O polyhedra in $Cs_2Mo_5O_{16}$ (left) and $Cs_2Mo_7O_{22}$ (right). The similarity between the polyhedra in both the structures should be apparent. The labelling of the atoms is consistent with Table 2. The coordinates of the cell outlines are $\frac{1}{4},0,0$; $\frac{1}{4},1,0$; $\frac{1}{4},1,1$ and $\frac{1}{4},0,1$ (left) and 0,0,0; 0,1,0; 1,1,1; and 1,0,1 (right). The diagram was produced by the use of *ORTEP* (Johnson, 1965).

tamolybdate study. No systematic variation could be detected in the intensities of the three reference reflexions. All 2744 unique reflexions with θ between 3·00 and 30·00° and with $k,l \geq 0$ were collected. Since the crystal was small ($\mu R \simeq 0{\cdot}1$) no absorption correction was applied, but apart from this the treatment of the intensities was the same as for the pentamolybdate. 982 reflexions with $I \leq 3\sigma(I)$ were given zero weight in the structure solution and refinement. The computer programs and scattering factors were the same as in the solution of the pentamolybdate.

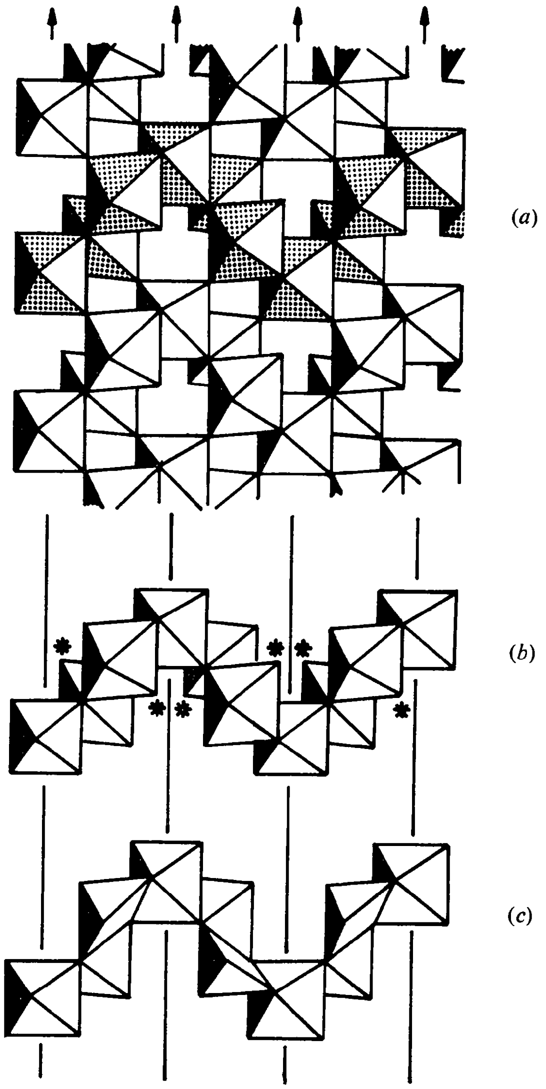

Fig. 4. The relationship between the 'predicted' structure for $Mo_3O_{10}^{2-}$ and the real $Mo_3O_{10}^{2-}$ chain as found in $Cs_2Mo_3O_{10}$. (*a*) The 'predicted' sheet structure. The chain of edge-sharing octahedra in the structure is shaded and reproduced in (*b*). This chain has stoichiometry Mo_3O_{12} and can be reduced to Mo_3O_{10} by removing the oxygens marked with an asterisk to give the chain of octahedra and square pyramids (*c*) which is found in the potassium, rubidium and caesium trimolybdates. Twofold axes are indicated by arrows. The chain found in the trimolybdates has the same symmetry as the 'parent' sheet structure.

Solution of the structure

The structure was solved in $C2/c$ by conventional Harker techniques. With all 'observed' reflexions given unit weight, two cycles of full-matrix least-squares refinement of all positions and isotropic temperature factors reduced R to 0·051. Successive cycles of block-diagonal least-squares refinement of all positional and thermal parameters, with metal atoms allowed to vary anisotropically and reflexions with $I > 3\sigma(I)$ weighted by $1/\sigma^2(F)$, gave $R = 0{\cdot}039$ and $R_w = 0{\cdot}043$. At this point all shifts were reduced to less than $0{\cdot}1\sigma$ and the refinement was terminated.* The final positional and thermal parameters are reported in Table 2. A difference map showed no features associated with the atom positions and all density was between $+2{\cdot}6$ and $-2{\cdot}9$ e Å^{-3}.

Description of the structure

The structure of $Cs_2Mo_7O_{22}$ is essentially the same as that of $Cs_2Mo_5O_{16}$ with the exception that the ReO_3-type strip of corner-sharing octahedra, which is five octahedra wide in the pentamolybdate, is seven octahedra wide in the heptamolybdate. The relationship between these two polymolybdates is shown in the *b*-axis projections (Fig. 2) and the diagram of the Mo–O frameworks (Fig. 1) of the two structures.

In the heptamolybdate the Mo–O sheets lie parallel to $(10\bar{1})$ and not (100) as in the pentamolybdate. This difference is due to the choice of the Dirichlet reduced cell in both cases. The alternative cell for the heptamolybdate, in which the Mo–O framework lies parallel to (100), is related to the cell used here by

$$\begin{pmatrix} \mathbf{a}_2 \\ \mathbf{b}_2 \\ \mathbf{c}_2 \end{pmatrix} = \begin{pmatrix} \bar{1} & 0 & 0 \\ 0 & \bar{1} & 0 \\ 1 & 0 & 1 \end{pmatrix} \begin{pmatrix} \mathbf{a}_1 \\ \mathbf{b}_1 \\ \mathbf{c}_1 \end{pmatrix} + \begin{pmatrix} \frac{1}{4} \\ -\frac{1}{4} \\ 0 \end{pmatrix} \begin{pmatrix} \mathbf{a}_1 \\ \mathbf{b}_1 \\ \mathbf{c}_1 \end{pmatrix}$$

where $\mathbf{a}_1$, $\mathbf{b}_1$, $\mathbf{c}_1$, $\mathbf{a}_2$, $\mathbf{b}_2$ and $\mathbf{c}_2$ are the vectors corresponding to the axes of the original and alternative cells respectively. The dimensions of the alternative cell are $a = 21{\cdot}54$, $b = 5{\cdot}537$, $c = 19{\cdot}524$ Å, $\beta = 125{\cdot}4°$. The principal differences between these dimensions and those of the pentamolybdate are the increased *c*-axis length and β angle, both of which are due to the increased width of the ReO_3-type strips which form the Mo–O framework.

The distortions in the Mo–O octahedra are the same as mentioned previously and give rise to Mo–O distances in the range 1·70 to 2·51 Å with average values of 1·97, 1·98, 2·01 and 1·99 Å for the octahedra around Mo(1) to Mo(4) respectively (Table 3).

In $Cs_2Mo_7O_{22}$, Cs is nine coordinate (Fig. 3). The coordination polyhedron is essentially the same as that in $Cs_2Mo_5O_{16}$. The distances to the oxygens which form the pentagon [$O(1)^{VII}$, $O(2)$, $O(5)^{VIIc}$, $O(6)$, $O(5)^{VII}$]

---

* See footnote on p. 1295.

and the distorted square [O(6)$^{\text{VII}}$, O(5), O(6)$^{\text{VIIc}}$, O(8)$^{\text{VI}}$] lie between 2·94 and 3·53 Å. Neither O(9), which forms the apex above the pentagon and is 3·71 Å from Cs, nor O(3)$^{\text{IVc}}$, which is 3·70 Å from Cs through the square face, is considered to be coordinated to Cs. As in the pentamolybdate the Cs–O polyhedra join through square faces to form chains. Because of the more extended Mo–O framework in $Cs_2Mo_7O_{22}$ the chains do not share common oxygens to form sheets as in $Cs_2Mo_5O_{16}$. As can be seen in Fig. 2, the Cs in the heptamolybdate occupy the same positions relative to the central Mo (twofold axis) of the seven octahedra wide strip as they do to the central Mo of the five octahedra wide strip in the pentamolybdate.

Discussion

$Cs_2Mo_5O_{16}$ and $Cs_2Mo_7O_{22}$ appear to be members of a series of compounds with general formula $A_2Mo_nO_{3n+1}$ (where A is a large alkali metal ion and n is a positive integer) which have Mo–O frameworks composed of sheets, n octahedra wide, of corner-linked octahedra joined together to form staggered sheets.

When n is odd, these sheets have twofold axes which are separated by $n/2$ octahedra (Figs. 1 and 2). The arrangement of octahedra between the twofold axes is the same as that found in the sheets of octahedra in MoO_3. The widths of adjacent strips of MoO_3-type structure are equal but the directions of edge-sharing of octahedra are perpendicular (related by the twofold axis). The Mo–O framework can therefore be described as strips of MoO_3 structure joined at planes of oxygen excess (the stoichiometry of the sheet is $MoO_{3+1/n}$). The obvious analogy is with shear structures where blocks of a particular structure type are joined at shear planes – planes of oxygen deficiency. As n is increased the distance between the twofold axes increases, so MoO_3 may be considered to be the limiting member ($n=\infty$) of the series.

Unpublished phase studies by the authors and work by Hoekstra (1973) have confirmed that no caesium polymolybdates higher than the heptamolybdate are formed. The structures of the penta- and heptamolybdates have been described here and the only remaining polymolybdate with n odd is $Cs_2Mo_3O_{10}$ which has a structure composed of chains of Mo–O octahedra and square pyramids (Gatehouse & Leverett, 1968). Although the trimolybdate chain does not conform to the scheme just proposed, it is very closely related. The 'predicted' Mo_3O_{10} framework is shown in Fig. 4(a). While this Mo–O framework is quite reasonable, there is no way in which a structure composed of these sheets can satisfy the coordination requirements of the relatively large proportion of Cs. The smaller proportions of Cs in the penta- and heptamolybdates can be accommodated because of the more extended nature of the Mo–O frameworks in these structures. The chain of edge-sharing octahedra which runs through the Mo_3O_{10} sheet [Fig. 4(b)] has stoichiometry Mo_3O_{12}. This can be reduced to Mo_3O_{10} by removing the oxygens marked in the diagram to form square pyramids. This chain, which retains the same symmetry as the Mo_3O_{10} sheet, is the chain found in $Cs_2Mo_3O_{10}$ and the isomorphous K and Rb trimolybdates.

Similar structures can be proposed for the cases when n is even; however the twofold axes are not retained and the width of the MoO_3-type strips alternate between $(n+1)/2$ and $(n-1)/2$ octahedra. $Cs_2Mo_2O_7$ probably has a chain structure for the same reason that $Cs_2Mo_3O_{10}$ has a chain structure. $Cs_2Mo_4O_{13}$ has not been prepared in a form suitable for X-ray single-crystal structure analysis and there are no other polymolybdates known to form with even n in the Cs_2MoO_4–MoO_3 system. There is, however, evidence to suggest that $Cs_2Mo_4O_{13}$ prepared by solid-state reaction of Cs_2MoO_4 and MoO_3 below 500°C forms with a chain structure similar to $K_2Mo_4O_{13}$ and its isomorph $Rb_2Mo_4O_{13}$ (Gatehouse & Leverett, 1971): Caillet & Saumagne (1969) reported that the infrared spectra of $Cs_2Mo_4O_{13}$ and $Rb_2Mo_4O_{13}$ were very similar. It would appear, then, that the $A_2Mo_nO_{3n+1}$ family is restricted to odd n.

The cell dimensions and density of $Rb_2Mo_7O_{22}$, a previously unreported phase, were obtained in the same way as those of the caesium polymolybdates and are reported in Table 1. This compound appears to be isomorphous with $Cs_2Mo_7O_{22}$; the slightly shorter a and c axes, and smaller β angle of the Rb compound are due to the smaller size of Rb which allows the Mo–O sheets, which are parallel to (101), to move closer together. The intersheet O–O distance which would be affected most by this movement would be that between O(5) and O(6) which is nearly perpendicular to (101) and is the shortest intersheet O–O distance in $Cs_2Mo_7O_{22}$ (3·30 Å). Assuming no 'slipping' of the Mo–O sheets relative to each other and no compensating distortions in the Mo–O framework, the corresponding distance in $Rb_2Mo_7O_{22}$ would be about 2·85 Å which is not prohibitively short. The structure may distort slightly to increase this distance.

As mentioned previously there are other rubidium polymolybdates which are isomorphous with the corresponding caesium polymolybdates: $Rb_2Mo_3O_{10}$ is isomorphous with $K_2Mo_3O_{10}$ and $Cs_2Mo_3O_{10}$; $Rb_2Mo_4O_{13}$ is isomorphous with $K_2Mo_4O_{13}$ and may be isomorphous with, or at least similar to, $Cs_2Mo_4O_{13}$. Salmon & Caillet (1969) have reported $Rb_2Mo_5O_{16}$ which, if it exists, may be expected to be isomorphous with $Cs_2Mo_5O_{16}$. There is no reason, from a structural point of view, why $Rb_2Mo_5O_{16}$ should not form with this structure. Nevertheless single crystals of this compound could not be prepared during these studies and Debye–Scherrer powder photographs have indicated that the major species forming at the pentamolybdate composition is $Rb_2Mo_4O_{13}$.

The fact that heptamolybdates are formed in the Cs and Rb systems while the highest polymolybdates in the Li and Na systems are $Li_2Mo_4O_{13}$ (Gatehouse &

Miskin, 1974) and $Na_6Mo_{10}O_{33}$ (Bolger & Gatehouse, 1973) is probably due to the size of the alkali metal ion; the larger Rb–O and Cs–O coordination polyhedra are able to accommodate a more extensive Mo–O framework.

In conclusion it may be noted that the $A_2Mo_nO_{3n+1}$ series reported here is in some ways analogous to the $M_xB_{2n}O_{4n+3}$ series reported by Galy & Lavaud (1971).

This work forms part of a project supported by the Australian Research Grants Committee. One of us (B.K.M.) acknowledges the receipt of a Commonwealth Postgraduate Research Award.

References

Bolger, C. & Gatehouse, B. M. (1973). Unpublished work.

Busing, W. R., Martin, K. O. & Levy, H. A. (1962). *ORFLS*. Oak Ridge National Laboratory Report ORNL-TM-305.

Caillet, P. & Saumagne, P. (1969). *J. Mol. Struct.* **4**, 351–359.

Cromer, D. T. & Waber, J. T. (1965). *Acta Cryst.* **18**, 104–109.

Galy, J. & Lavaud, D. (1971). *Acta Cryst.* **B27**, 1005–1009.

Gatehouse, B. M. (1974). *J. Less-Common Met.* **36**, 53–57.

Gatehouse, B. M. & Leverett, P. (1968). *J. Chem. Soc.* (*A*), pp. 1398–1405.

Gatehouse, B. M. & Leverett, P. (1971). *J. Chem. Soc.* (*A*), pp. 2107–2112.

Gatehouse, B. M. & Miskin, B. K. (1974). *J. Solid State Chem.* **9**, 247–253.

Hoekstra, H. R. (1973). *Inorg. Nucl. Chem. Lett.* **9**, 1291–1301.

International Tables for X-ray Crystallography (1959). Vol. II. Birmingham: Kynoch Press.

Johnson, C. K. (1965). *ORTEP*. Oak Ridge National Laboratory Report ORNL-3794.

Salmon, R. & Caillet, P. (1969). *Bull. Soc. Chim. Fr.* pp. 1569–1573.

Shiono, R. (1968). *Block-Diagonal Least-Squares Refinement Program*, Department of Crystallography, Univ. of Pittsburgh.

Spitsyn, V. & Kuleshov, I. M. (1951). *Zh. Obshch. Khim.* **21**, 1372. Phase diagram reproduced by E. M. Levin, C. R. Robbins & H. F. McMurdie (1964). *Phase Diagrams for Ceramists*, edited by M. K. Reser, p. 86. The American Ceramic Society.

White, J. C. B. (1965). Melbourne Univ. Fourier Summation Program, *MUFR*3. See J. S. Rollett (1961) in *Computing Methods and the Phase Problem in X-ray Crystal Analysis*, edited by Pepinsky, Robertson & Speakman, p. 87. Oxford: Pergamon Press.

Acta Cryst. (1975). B**31**, 1299

The Crystal and Molecular Structure of [4,4,2]Propella-3,8-diene-11,12-dione

By R. Fink,* Dick van der Helm† and S. C. Neely

University of Oklahoma, Chemistry Department, Norman, Oklahoma 73069, *U.S.A.*

(*Received* 31 *October* 1974; *accepted* 23 *December* 1974)

The crystal structure of the title compound has been determined and refined by three-dimensional least-squares calculations to a final R value of 0·057 using 1870 counter data. The compound crystallizes in the monoclinic space group $P2_1/c$ with $a=7{\cdot}438$, $b=11{\cdot}539$, $c=12{\cdot}935$ Å and $\beta=116{\cdot}22°$. There are four $C_{12}H_{12}O_2$ molecules in the unit cell. The molecule possesses nearly mm symmetry with the two six-membered rings in the boat form and folded toward the diketone.

Introduction

The structure of [4,4,2]propella-3,8-diene-11,12-dione was determined as part of a study of the effects of π electrons on $n \rightarrow \pi^*$ transition energies of *cis*-α-diketones (Neely, Fink, van der Helm & Bloomfield, 1971). The visible and ultraviolet solution absorption spectra of this compound as well as its di- and tetrahydro derivatives have been reported (Bloomfield & Moser, 1968). The title compound and the dihydro derivative show $n \rightarrow \pi^*$ absorption at unusually long wavelengths compared with other unsubstituted α-diketones (Birnbaum, Cookson & Lewin, 1961; Leonard & Mader, 1950; Alder, Schafer, Esser, Krieger & Reubke, 1955). Theoretical studies show that the transition energies depend on the molecular conformations (Fink, 1973; Neely, Fink, van der Helm & Bloomfield, 1971). The structure of the title compound was determined to obtain bond-length and bond-angle data necessary for the calculations and possible clues about preferred conformations of these molecules in solution.

---

* Supported by a National Aeronautics and Space Administration Predoctoral Traineeship. Present address: Chemistry Department, Oklahoma City University, Oklahoma City, Oklahoma 73106.

† Supported by N.I.H. Development Award K4-GM-42572.